Supplementary Materials for Full-dimensional quantum mechanics calculations for the spectroscopic characterization of the isomerization transition states of HOCO/DOCO systems

Dandan Ma[1], Haisheng Ren[2] and Jianyi Ma[1]**

[1]*Institute of Atomic and Molecular Physics, Sichuan University, Chengdu, Sichuan 610065, China*

[2]*School of Chemical Engineering, Sichuan University, Chengdu, Sichuan 610065, China*

Supplementary Materials

Coordinates system

Diatom-diatom Jacobi coordinates were used, which include six coordinates, r_0, r_1, r_2, θ_1, θ_2 and ϕ, as depicted in Fig. S1. In detail, r_1 and r_2 refer to the diatomic bond lengths of HO and CO, respectively, while r_0 represents the distance between the two centers of mass. $\theta_1(\theta_2)$ is the Jacobi angular coordinate between vectors $\vec{r}_0$ and $\vec{r}_1(\vec{r}_2)$, with the out-of-plane torsion angle is given by ϕ.

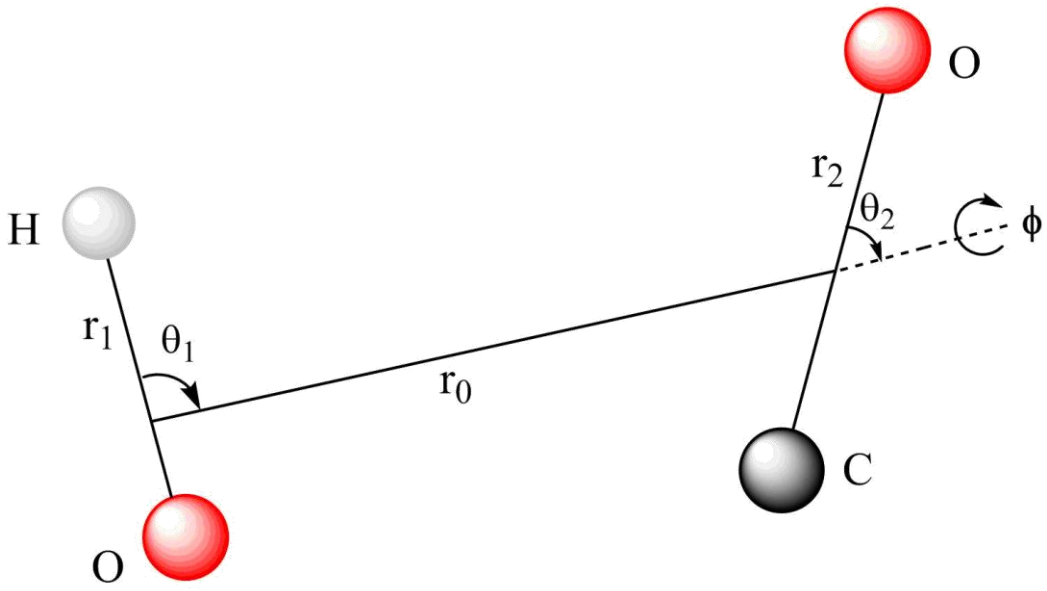

Figure S1. Jacobi coordinates used to describe the diatom-diatom HOCO system.

Potential energy surface

The highly accurate full-dimensional global PES for HOCO (and its deuterated isotopomer DOCO) used in our work was developed by Li *et al*. using about 75000 *ab initio* points which were calculated using a definitely corrected couple cluster with singles, doubles, and perturbative triples with the augmented correlation-consistent polarized valence triple-zeta basis set (CCSD(T)-F12a/AVTZ).[1, 2] The permutation invariant polynomial neural network (PIP-NN) approach was employed to fit these points which were assigned in three regions, i.e., the OH + CO entrance channel region, the H + CO_2 exit channel region and the HOCO interaction region. The

PIP-NN method refers to adapting the permutation symmetry rigorously in the NN fitting. That is to say the low-order PIPs also were included in the input layer of the NNs. They are symmetrized monomials,[3]

$$G=\hat{S}\prod_{i<j}^{N} p_{ij}^{l_{ij}} \tag{1}$$

where $\hat{S}$ is the symmetrization operator, containing all possible systemic nuclear permutation operations. $p_{ij}=\exp(-ar_{ij})$ represent the Morse-like variables with a is an constant changeable and r_{ij} are the $N(N-1)/2$ internuclear distances. Besides, l_{ij} is the degree of p_{ij} and

$$M=\sum_{i<j}^{N} l_{ij} \tag{2}$$

is the total degree in each monomial. In the input layer, the number of PIPs should be sufficiently large in order to ensure the permutation symmetry of the system[4]. In this fitting, all 17 PIPs up to the second order had been included.

Some of the NN structures in different region with one or two hidden layers were tested, especially the HOCO interaction region as the complex structure of PES. Two hidden layers with N_1 and N_2 neurons are settled. The *ab initio* data is divided into three sets in each NN fitting, i.e., the training, validation, and test set including 90%, 5%, and 5% of the data points respectively. The Levenberg Marquardt algorithm[5] was employed in all of the NN fittings, and the root mean square error (RMSE) was given by:

$$\text{RMSE}=\sqrt{\sum_{i=1}^{N_{\text{data}}}(E_{\text{fitted}}-E_{\text{ab}})^2/N_{\text{data}}} \tag{3}$$

where E_{fitted} and E_{ab} are respectively the fitted energy and the *ab initio* energy. Fits with similar RMSEs for all three sets were selected to avoid false extrapolation. The maximum deviation also as evaluation criteria was used to select the final PIP-NN fits. Following the NN ensemble approach, the final PIP-NN PES was obtained by averaging the three best fits to minimize random errors.[6] At last, switch functions

were employed to connect the three regions.

Details for the finally fitting were listed. For the OH + CO region, 1021 parameters and a two-layer NN structure, (N1–N2) = (20–30), were used. Meanwhile, the final NN structure in H + CO_2 region has a single-layer, (N1–N2) = (10–0), with 761 parameters. For the important HOCO region, a two layers NN structure, (N1–N2) = (50–80), with 5061 parameters were employed in the final fitting. Thus the RMSE and the maximum deviation of the total PES are 5.0 meV and 209.4 meV, respectively. While, for points of energies less than 3.0 eV (relative to the global minimum), the corresponding values are separately 3.0 meV and 127.7 meV.

Lanczos algorithm

Lanczos algorithm[7] was used to calculate the eigenvalues and wavefunctions of the HOCO system, where the related six-dimensional (6D) non-rotating (J=0) Hamiltonian ($\hbar$=1) on the basis of the above coordinate system is defined as follows,

$$\hat{H} = \sum_{i=0}^{1}\left(-\frac{1}{2\mu_i}\frac{\partial^2}{\partial r_i^2}\right) + \left(-\frac{1}{2\mu_2}\frac{\partial^2}{\partial r_2^2} + V_2(r_2)\right) + \sum_{i=0}^{2}\frac{\hat{j}_i^2}{2\mu_i r_i^2} + \left[V(r_0,r_1,r_2,\theta_1,\theta_2,\phi) - \sum_{i=0}^{2} V_i(r_i)\right] \quad (4)$$

where μ_i are the reduced masses of the radial coordinates, V is the PES mentioned above, and V_i is the reference potential along the corresponding radial coordinates. $\hat{j}_1$, $\hat{j}_2$ serve as the angular momentum operators corresponding to θ_1, θ_2. It is should be noted that $\hat{j}_0^2 = (\hat{j}_1 + \hat{j}_2)^2$.For the wavefunctions, the potential-optimized discrete variable representation (PODVR)[8, 9] was used to describe the three radial coordinates, and the uncoupled spherical harmonics basis was adopted to describe the angular directions,

$$|j_1 m_1 j_2 m_2\rangle = |j_1 m_1\rangle|j_2 m_2\rangle = Y_{j_1 m_1}(\theta_1) Y_{j_2 m_2}(\theta_2)\Phi_{m_1}(\phi) \quad (5)$$

where Y are spherical harmonics functions, Φ are Fourier functions, and m are the azimuthal quantum numbers.[10]The Lanczos states $|\psi_k\rangle$ were derived from the

iteration of the normalized initial state of $|\psi_1\rangle$ using the following three-term recursion formula,

$$|\psi_{k+1}\rangle = \beta_k^{-1}\left[\hat{H}|\psi_k\rangle - \alpha_k|\psi_k\rangle - \beta_{k\text{-}1}|\psi_{k\text{-}1}\rangle\right],\ k=1, 2 \cdots \tag{6}$$

where $\hat{H}$ is the Hamiltonian and α_k and β_k represent the diagonal and sub/super-diagonal elements of the tridiagonal Lanczos matrix, respectively, given by

$$\alpha_k = \langle\psi_k|\hat{H}\psi_k - \beta_{k\text{-}1}\psi_{k\text{-}1}\rangle$$

$$\beta_k = \langle\hat{H}\psi_k - \alpha_k\psi_k - \beta_{k\text{-}1}\psi_{k\text{-}1}|\hat{H}\psi_k - \alpha_k\psi_k - \beta_{k\text{-}1}\psi_{k\text{-}1}\rangle^{\frac{1}{2}} \tag{7}$$

$$\beta_0 = 0$$

By diagonalizing the $K\times K$ Lanczos matrix, we can obtain the eigenvectors $\left\{Z_i^{(k)} = \left[z_{li}^{(k)}, \cdots, z_{ki}^{(k)}, \cdots, z_{Ki}^{(K)}\right]^T\right\}$ as well as the corresponding eigenvalues $\left\{E_i^{(k)}\right\}$ of the given iteration step K. Subsequently, the wavefunctions can be expressed as a linear combination of eigenvectors and iterative Lanczos states, namely, $\left|E_i^{(k)}\right\rangle = \sum_{K=1}^{K} z_{ki}^{K}|\psi_k\rangle$. Hence, the smallness of the last element of the Lanczos eigenvector, i.e., $\left|z_{Ki}^{(K)}\right|$, becomes the decisive factor for the convergence of the Lanczos iteration.

We listed pure torsional states of *trans*-HOCO, *cis*-HOCO, *trans*-DOCO and *cis*-DOCO which were used in the calculation and fit of effective frequencies in Table S5. It should be noted that all of the levels belong to a species were used in the fitted curves 1, except the level of *trans*-HOCO marked in red. In the fitted curves 2, the levels marked in blue were not included.

Table S1. Parameters in the calculations of the HOCO (DOCO) system

Parameters	HOCO	DOCO
Grid/basis ranges and sizes	$r_0 \in (1.5, 7.5)$, $N_0 = 10$ $r_1 \in (1.1, 4.5)$, $N_1 = 4$ $r_2 \in (1.2, 5.0)$, $N_2 = 6$ PODVR for r_0, r_1, r_2	$r_0 \in (1.5, 7.5)$, $N_0 = 10$ $r_1 \in (1.1, 4.5)$, $N_1 = 5$ $r_2 \in (1.2, 5.0)$, $N_2 = 5$ PODVR for r_0, r_1, r_2
Largest values of j_1	55	55
Largest values of j_2	80	80
Largest values of m	55	55
Lanczos steps	25000	25000

Table S2. Fundamental vibrational frequencies (in cm^{-1}) for both *trans*- and *cis*-DOCO

	trans-DOCO				*cis*-DOCO			
mode	This work	Theo.[a]	Theo.[b]	Exp.[m]	This work	Theo.[a]	Theo.[b]	Exp.[m]
v_1, O-D stretch	2684.60	2691	2685.1	2558[e],2684.10[k], 2678.1[g]	2544.71	2558	2551.6	2456[e],
v_2, C-O' stretch	1850.19	1859	1859.8	1825[e],1851.65[h], 1846.2[g]	1818.17	1829	1827.5	1798[e],
v_3, D-O-C bend	1080.27	1092	1086.4	1117[e], 1145[i] , 1082.6[g]	1118.81	1132	1123.1	1148[e], 1081[i]
v_4, O-C stretch	898.09	906	902.6	…	956.19	961	960.9	…
v_5, O-C-O' bend	586.98	593	590.1	557[i]	535.79	539	539.8	563[e], 597[i]
v_6, torsion	392.77	396	368.0	472[e]	456.55	452	446.9	497[e]

[a] Reference 11, [b] Reference 12, [e] Reference 13, [g] Reference 14, [h] Reference15, [i] Reference16, [k] Reference17

Table S3. Energy and assignments of vibrational levels of *trans*-HOCO and *cis*-HOCO up to 3500 cm^{-1}

	trans-HOCO						*cis*-HOCO			
NO.	Energy	states	Energy	states	Energy	states	Energy	states	Energy	states
1	0	6^0	2453.54	$6^0 5^4$	3066.07	$6^0 5^2 2^1$	527.24	6^0	2991.88	$6^0 5^2 3^1$
2	502.78	6^1	2458.27	$6^0 5^1 2^1$	3070.01	$6^0 5^5$	1074.84	6^1	3056.16	$6^3 4^1$
3	611.84	$6^0 5^1$	2467.72	$6^3 4^1$	3078.89	$6^3 5^1 4^1$	1122.16	$6^0 5^1$	3058.74	$6^0 3^2$
4	982.22	6^2	2485.77	$6^4 5^1$	3088.13	$6^0 4^3$	1565.16	$6^0 4^1$	3124.97	$6^1 4^2$
5	1048.04	$6^0 4^1$	2570.28	$6^1 4^2$	3108.12	$6^4 5^2$	1582.87	6^2	3171.93	$6^0 4^2 5^1$
6	1118.56	$6^1 5^1$	2595.0	6^6	3168.04	$6^1 5^1 4^2$	1669.69	$6^1 5^1$	3189.62	$6^2 5^1 4^1$
7	1436.80	6^3	2626.20	$6^3 3^1$	3206.28	$6^2 4^1 3^1$	1719.63	$6^0 5^2$	3272.77	$6^3 3^1$
8	1204.33	$6^0 3^1$	2671.28	$6^0 5^1 4^2$	3221.61	$6^6 5^1$	1799.65	$6^0 3^1$	3322.83	6^9
9	1224.99	$6^0 5^2$	2627.81	$6^2 5^1 4^1$	3234.91	$6^2 5^2 4^1$	2042.61	6^3	3348.90	$6^0 5^3 4^1$
10	1546.59	$6^1 4^1$	2679.23	$6^3 5^2$	3246.47	$6^3 5^1 3^1$	2109.13	$6^1 4^1$	3362.14	$6^2 5^3$
11	1600.83	$6^2 5^1$	2739.20	$6^1 4^1 3^1$	3259.42	$6^0 4^2 3^1$	2155.02	$6^0 5^1 4^1$	3363.51	$6^0 4^1 2^1$
12	1651.56	$6^0 5^1 4$	2761.61	$6^1 5^2 4^1$	3271.11	$6^0 5^2 4^2$	2172.93	$6^2 5^1$	3365.73	$6^1 4^1 3^1$
13	1705.08	$6^1 3^1$	2790.96	6^7	3288.04	$6^5 4^1$	2267.14	$6^1 5^2$	3389.26	$6^2 2^1$
14	1734.90	$6^1 5^2$	2795.58	$6^2 5^1 3^1$	3299.402	$6^3 5^3$	2320.30	$6^0 5^3$	3407.22	$6^0 5^1 4^1 3^1$
15	1812.21	$6^0 5^1 3$	2826.38	$6^2 5^3$	3343.27	$6^1 5^1 4^1 3^1$	2341.89	$6^0 2^1$	3429.75	$6^2 5^1 3^1$
16	1838.86	$6^0 5^3$	2834.85	$6^2 2^1$	3353.04	$6^2 3^2$	2348.86	$6^1 3^1$	3463.67	$6^4 4^1$
17	1852.12	$6^0 2^1$	2842.58	$6^0 5^1 4^1 3$	3370.46	$6^1 5^3 4^1$	2394.31	$6^0 5^1 3^1$	3472.80	$6^1 5^4$
18	1861.93	6^4	2864.92	$6^0 5^3 4^1$	3372.36	$6^1 4^1 2^1$	2459.03	6^4	3475.57	$6^1 5^1 2^1$
19	2019.34	$6^2 4^1$	2876.06	$6^5 5^1$	3412.36	$6^5 3^1$	2587.99	$6^0 4^2$		
20	2058.38	$6^3 5^1$	2878.27	$6^0 4^1 2^1$	3416.53	$6^0 3^2 4^1$	2608.37	$6^2 4^1$		
21	2076.38	$6^0 4^2$	2885.88	$6^1 3^2$	3437.97	$6^2 5^2 3^1$	2696.14	$6^1 5^1 4^1$		
22	2153.67	$6^1 5^1 4$	2886.19	$6^4 4^1$	3442.36	$6^0 5^2 4^1 3^1$	2748.58	$6^0 5^2 4^1$		
23	2179.10	$6^2 3^1$	2931.54	$6^1 5^2 3^1$	3453.63	$6^2 5^4$	2765.65	$6^2 5^2$		
24	2218.82	$6^2 5^2$	2966.79	6^8	3475.23	$6^0 5^4 4^1$	2817.43	$6^0 4^1 3^1$		
25	2241.77	$6^0 4^1 3$	2969.55	$6^1 5^4$	3476.43	$6^0 5^1 4^1 2^1$	2843.94	$6^2 3^1$		
26	2251.07	6^5	2994.00	$6^0 5^1 3^2$	3478.56	$6^3 4^2$	2867.56	$6^1 5^3$		
27	2257.44	$6^0 5^2 4$	3031.32	$6^0 5^3 3^1$	3497.60	$6^1 5^1 3^2$	2887.98	$6^1 2^1$		
28	2318.15	$6^1 5^1 3$	3035.78	$6^2 4^2$	3498.70	$6^4 5^1 4^1$	2924.92	$6^0 5^4$		
29	2352.30	$6^1 5^3$	3040.52	$6^4 3^1$	3497.60	$6^1 5^1 3^2$	2929.81	$6^0 5^1 2^1$		
30	2387.78	$6^0 3^2$	3050.07	$6^0 3^1 2^1$	3498.70	$6^4 5^1 4^1$	2942.67	$6^1 5^1 3^1$		
31	2421.02	$6^0 5^2 3$					2966.79			

Table S4. Energy and assignments of vibrational levels of *trans*-DOCO and *cis*-DOCO up to 3500 cm^{-1}

	trans-DOCO						*cis*-DOCO			
NO.	Energy	states	Energy	states	Energy	states	Energy	states	Energy	states
1	0	6^0	2454.11	$6^5 5^1$	3071.51	$6^1 1^1$	564.42	6^0	3109.13	$6^0 1^1$
2	392.77	6^1	2469.37	$6^1 5^2 4^1$	3080.35	$6^3 4^1 3^1$	1020.97	6^1	3138.70	$6^0 5^3 4^1$
3	587.04	$6^0 5^1$	2519.53	$6^1 3^2$	3082.61	$6^7 5^1$	1100.21	$6^0 5^1$	3164.11	$6^0 5^1 4^1 3^1$
4	773.69	6^2	2542.62	$6^0 5^1 4^1 3^1$	3090.31	6^{10}	1451.47	6^2	3175.79	$6^4 4^1$
5	898.09	$6^0 4^1$	2546.33	$6^4 3^1$	3096.05	$6^1 5^1 3^2$	1520.62	$6^0 4^1$	3179.05	$6^1 5^4$
6	985.65	$6^1 5^1$	2550.57	$6^2 4^2$	3118.06	$6^0 5^2 4^1 3^1$	1554.12	$6^1 5^1$	3205.82	$6^1 5^2 3^1$
7	1080.26	$6^0 3^1$	2567.97	$6^2 5^3$	3131.65	$6^1 4^1 2^1$	1641.77	$6^0 5^2$	3226.94	$6^1 3^2$
8	1141.24	6^3	2619.81	$6^2 2^1$	3145.39	$6^4 5^1 3^1$	1683.23	$6^0 3^1$	3246.78	$6^4 5^2$
9	1173.94	$6^0 5^2$	2631.44	$6^3 5^1 4^1$	3165.90	$6^2 5^4$	1861.36	6^3	3265.51	$6^2 2^1$
10	1288.65	$6^1 4^1$	2636.52	$6^1 5^2 3^1$	3175.99	$6^0 3^3$	1974.39	$6^1 4^1$	3276.18	$6^0 5^5$
11	1371.89	$6^2 5^1$	2650.19	$6^0 5^3 4^1$	3185.30	$6^6 3^1$	1978.78	$6^2 5^1$	3303.97	$6^3 5^1 4^1$
12	1467.27	$6^1 3^1$	2664.96	$6^0 4^3$	3212.73	$6^2 5^1 2^1$	2053.63	$6^0 5^1 4^1$	3307.14	$6^0 5^3 3^1$
13	1482.31	$6^0 5^1 4^1$	2684.60	$6^0 1^1$	3220.80	$6^1 5^3 3^1$	2092.40	$6^1 5^2$	3325.54	$6^2 4^2$
14	1493.73	6^4	2686.60	6^8	3225.59	$6^1 4^2 3^1$	2132.37	$6^1 3^1$	3327.75	$6^0 5^1 3^2$
15	1578.46	$6^1 5^2$	2706.47	$6^4 5^2$	3232.17	$6^3 5^2 4^1$	2189.86	$6^0 5^3$	3347.59	6^9
16	1659.24	$6^0 5^1 3^1$	2708.77	$6^5 4^1$	3234.21	$6^0 5^4 4^1$	2215.13	$6^0 5^1 3^1$	3397.53	$6^0 4^3$
17	1666.67	$6^2 4^1$	2709.27	$6^0 5^1 3^2$	3241.55	$6^3 3^2$	2248.34	6^4	3427.06	$6^3 5^3$
18	1744.14	$6^3 5^1$	2723.18	$6^2 4^1 3^1$	3243.17	$6^0 5^1 4^3$	2375.18	$6^3 5^1$	3436.41	$6^1 5^1 4^2$
19	1760.67	$6^0 5^3$	2743.15	$6^0 4^1 2^1$	3253.52	$6^4 4^2$	2382.59	$6^0 2^1$	3441.68	$6^2 5^2 4^1$
20	1786.19	$6^0 4^2$	2762.00	$6^1 5^1 4^2$	3268.58	$6^0 5^1 1^1$	2395.49	$6^2 4^1$	3455.58	$6^0 5^2 2^1$
21	1829.21	6^5	2763.98	$6^1 5^4$	3280.14	$6^0 5^2 3^2$	2464.76	$6^0 4^2$	3458.51	$6^3 5^1 3^1$
22	1841.82	$6^2 3^1$	2771.21	$6^6 5^1$	3291.77	$6^7 4^1$	2502.27	$6^1 5^1 4^1$	3485.20	$6^2 4^1 3^1$
23	1850.19	$6^0 2^1$	2796.80	$6^3 5^1 3^1$	3297.63	$6^1 3^1 2^1$	2510.03	$6^2 5^2$	3487.93	$6^0 3^1 2^1$
24	1879.07	$6^1 5^1 4^1$	2816.51	$6^0 5^3 3^1$	3310.26	$6^2 5^1 4^1 3^1$	2554.54	$6^2 3^1$		
25	1966.92	$6^0 4^1 3^1$	2828.60	$6^1 5^1 2^1$	3317.26	$6^4 5^3$	2594.99	$6^0 5^2 4^1$		
26	1969.98	$6^2 5^2$	2843.26	$6^0 4^2 3^1$	3321.97	$6^1 5^1 4^1 2^1$	2610.56	6^5		
27	2030.58	$6^3 4^1$	2858.43	$6^2 5^2 4^1$	3326.13	$6^5 5^1 4^1$	2628.05	$6^0 4^1 3^1$		
28	2051.95	$6^1 5^1 3^1$	2877.45	$6^5 3^1$	3330.88	$6^8 5^1$	2636.90	$6^1 5^3$		
29	2066.33	$6^0 5^2 4^1$	2887.77	$6^2 3^2$	3335.53	$6^4 2^1$	2660.66	$6^1 5^1 3^1$		
30	2099.72	$6^4 5^1$	2909.81	$6^3 4^2$	3349.74	$6^1 5^2 4^2$	2735.95	$6^0 5^4$		
31	2138.31	$6^0 3^2$	2913.31	$6^0 3^1 2^1$	3356.79	$6^1 5^5$	2767.73	$6^0 5^2 3^1$		
32	2146.25	6^6	2919.94	6^9	3390.67	$6^3 5^2 3^1$	2785.22	$6^0 3^2$		
33	2171.18	$6^1 5^3$	2933.43	$6^1 5^1 4^1 3^1$	3394.20	$6^1 4^1 3^2$	2795.64	$6^3 4^1$		
34	2174.36	$6^1 4^2$	2933.70	$6^0 5^5$	3394.77	$6^0 5^4 3^1$	2837.30	$6^1 2^1$		
35	2202.66	$6^3 3^1$	2948.57	$6^0 5^2 4^2$	3398.98	$6^6 5^2$	2865.63	$6^3 5^2$		
36	2238.01	$6^0 5^2 3^1$	2949.46	$6^3 5^3$	3415.61	$6^0 5^1 4^2 3^1$	2910.90	$6^2 5^1 4^1$		
37	2240.93	$6^1 2^1$	2982.64	$6^4 5^1 4^1$	3416.28	$6^1 5^2 2^1$	2915.06	$6^1 4^2$		
38	2262.64	$6^2 5^1 4^1$	2985.25	$6^3 2^1$	3418.36	$6^4 4^1 3^1$	2916.09	$6^0 5^1 2^1$		
39	2346.89	$6^3 5^2$	3013.27	$6^0 5^2 2^1$	3424.89	$6^2 4^3$	2946.41	6^6		
40	2347.23	$6^0 5^4$	3015.31	$6^0 4^1 3^2$	3447.33	$6^2 1^1$	2954.62	$6^3 3^1$		
41	2351.61	$6^1 4^1 3^1$	3018.82	$6^6 4^1$	3454.11	$6^2 5^3 4^1$	2994.71	$6^0 5^1 4^2$		
42	2367.41	$6^0 5^1 4^2$	3021.60	$6^2 5^2 3^1$	3454.54	$6^7 3^1$	3034.48	$6^1 5^2 4^1$		
43	2378.68	$6^4 4^1$	3037.42	$6^5 5^2$	3469.08	$6^2 5^1 3^2$	3041.92	$6^2 5^3$		
44	2423.79	6^7	3050.64	$6^1 4^3$	3486.56	$6^5 5^1 3^1$	3057.34	6^7		
45	2430.57	$6^2 5^1 3^1$	3059.60	$6^1 5^3 4^1$	3486.66	$6^0 5^1 4^2 3^1$	3073.12	$6^1 4^1 3^1$		

Table S5. Pure torsional states of *trans*-HOCO, *cis*-HOCO, *trans*-DOCO and *cis*-DOCO

level	*trans*-HOCO	*cis*-HOCO	*trans*-DOCO	*cis*-DOCO
6^0	0	527.24	0	564.42
6^1	502.78	1074.84	392.77	1020.97
6^2	982.22	1582.87	773.69	1451.47
6^3	1436.80	2042.61	1141.24	1861.36
6^4	1861.93	2459.03	1493.73	2248.34
6^5	2251.07	2790.96	1829.21	2610.56
6^6	2595.0	2966.79	2146.25	2946.41
6^7	2790.96		2423.79	3057.34
6^8	2966.79		2686.60	
6^9			2919.94	
6^{10}			3090.31	

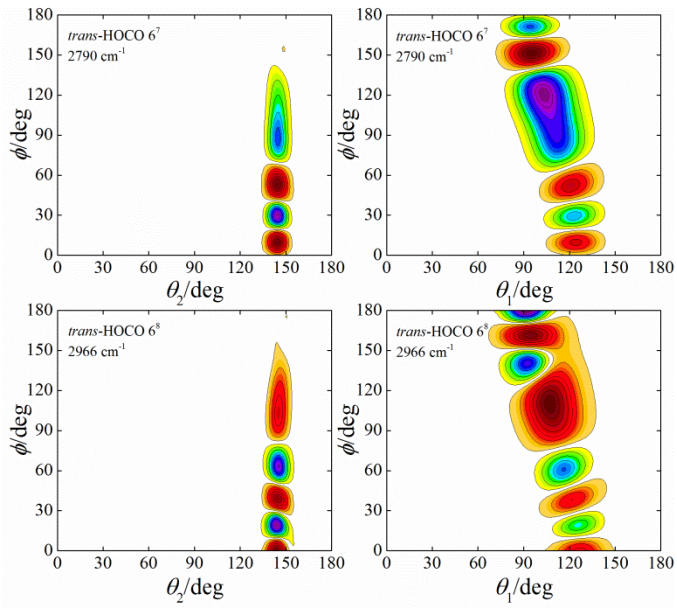

Figure S2. Wavefunctions of the *trans*-$6^7/6^8$ states shown in the (θ_2, ϕ) and (θ_1, ϕ) planes; the remaining four coordinates take the equilibrium values of *trans*-HOCO.

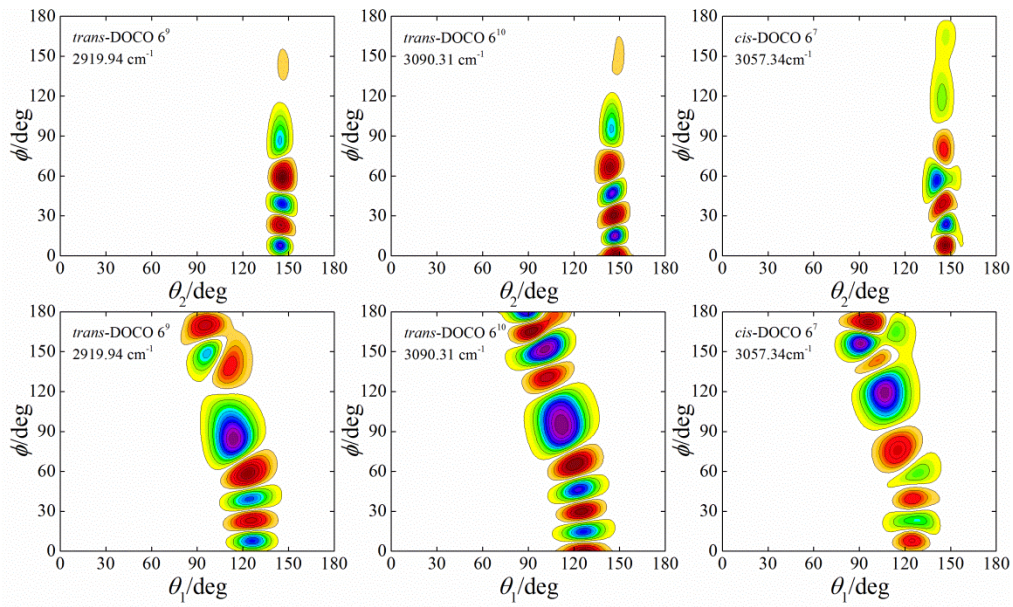

Figure S3. Wavefunctions of the *trans*-$6^9/6^{10}$ and *cis*-6^7 states shown in the (θ_2, ϕ) and (θ_1, ϕ) planes; the remaining four coordinates take the equilibrium values of *trans*-DOCO.

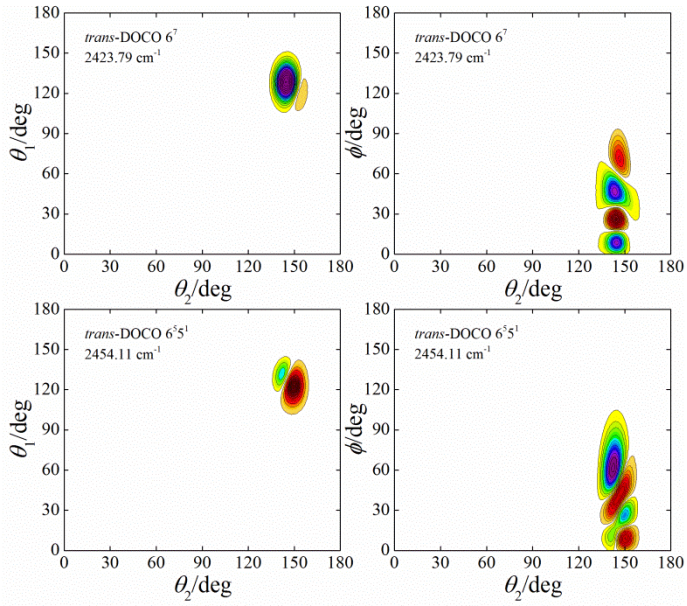

Figure S4. Wavefunctions of the *trans*-6^7 and *trans*-$6^5 6^1$ states shown in the (θ_2, θ_1) and (θ_2, ϕ) planes; the remaining four coordinates take the equilibrium values of *trans*-DOCO.

References

1. J. Li, J. Chen, D. H. Zhang and H. Guo, *J. Chem. Phys.*, 2014, **140**, 044327.
2. J. Chen, X. Xu, X. Xu and D. H. Zhang, *J Chem Phys*, 2013, **138**, 221104.
3. Z. Xie and J. M. Bowman, *J. Chem. Theor. Comput.*, 2010, **6**, 26.
4. J. Li, B. Jiang and H. Guo, *J Chem Phys*, 2013, **139**, 204103.
5. M. T. Hagan and M. B. Menhaj, *IEEE Trans. Neural Networks* 1994, **5**, 989.
6. Z.-H. Zhou, J. Wu and W. Tang, *Art. Intel.*, 2002, **137**, 239.
7. H. Guo, *Rev. Comput. Chem.*, 2007, **25**, 285-347.
8. J. Echave and D. C. Clary, *Chem. Phys. Lett.*, 1992, **190**, 225.
9. H. Wei and T. Carrington Jr., *J. Chem. Phys.*, 1992, **97**, 3029.
10. R. Chen, G. Ma and H. Guo, *J. Chem. Phys.*, 2001, **114**, 4763-4774.
11. M. Mladenović, *J. Phys. Chem. A*, 2013, **117**, 7224-7235.
12. X. Huang, R. C. Fortenberry, Y. Wang, J. S. Francisco, T. D. Crawford, J. M. Bowman and T. J. Lee, *J. Phys. Chem. A*, 2013, **117**, 6932–6939.
13. D. E. Milligan and M. E. Jacox, *J. Chem. Phys.*, 1971, **54**, 927-942.
14. D. Forney, M. E. Jacox and W. E. Thompson, *J. Chem. Phys.*, 2003, **119**, 10814-10823.
15. T. J. Sears, W. M. Fawzy and P. M. Johnson, *J. Chem. Phys.*, 1992, **97**, 3996-4007.
16. T. Oyama, W. Funato, Y. Sumiyoshi and Y. Endo, *J. Chem. Phys.*, 2011, **134**, 174303.
17. J. T. Petty and C. B. Moore, *J. Chem. Phys.*, 1993, **99**, 47.